

## **CARBONATION RATES OF ALKALI-ACTIVATED AND CEMENT-BASED CONCRETES**

**Marija Nedeljković (1, 2), Kamel Arbi (3), Guang Ye (1)**

(1) Microlab, Department of 3MD, Faculty of Civil Engineering and Geosciences, Delft University of Technology, The Netherlands

(2) TNO Buildings, Infrastructure & Maritime Delft, The Netherlands

(3) Delta Concrete Consult B.V. Vianen, The Netherlands

### **Abstract**

The reduction of pH from ~12.5 to ~9 by carbonation of the pore solution of reinforced cement-based concrete structures results in the reinforcement corrosion. The rate of carbonation is an important input for design of the concrete cover depth and the service life prediction of reinforced concrete structures because the initiation of reinforcement corrosion is usually considered as the end of service life of concrete infrastructure. The information from the field carbonation of alkali activated concrete is in most cases limited and related to exposure shorter than 40 years. In this paper, a comparative study regarding accelerated and natural carbonation of alkali-activated concretes and cement-based concretes has been carried out. The pH and carbonation depths are periodically measured. The results show that, despite the low porosity of alkali-activated concrete with 50 wt. % slag, these concretes must have an appropriate curing in order to be used in exposure classes where carbonation is an issue, due to their lower carbonation resistance compared to cement-based concrete. Regardless the exposure conditions, the pH of carbonated alkali-activated concrete was maintained above 9. Finally, recommendations for alkali activated concrete applications and their improved carbonation resistance are given.

Keywords: Alkali activated concrete, Carbonation, Natural test, Accelerated test, pH

### **1. INTRODUCTION**

Structural application of alkali activated concrete is still argued worldwide due to lack of data regarding long-term performance [1]. Additionally, the prediction of the service life of structures made with alkali activated concrete is not reported in the literature. This largely impedes the standardization process of alkali activated concrete for the building industry. Furthermore, it is still unknown whether the carbonation is responsible for corrosion of

reinforcing steel in alkali-activated concretes or whether some other carbonation-induced structural deterioration of the alkali-activated binder has to be envisaged.

Carbonation of cement-based concrete results in a decrease of the pH of the pore solution, initiating the corrosion of reinforcing steel. Beside carbonation of the pore solution, the carbonation of  $\text{Ca(OH)}_2$  and C-S-H gel result in the formation of  $\text{CaCO}_3$  and amorphous silica gel, respectively. Figure 1 demonstrates influence of key parameters on the carbonation mechanism for two concrete domains, i.e. pore solution and microstructure. The comparative study of cement and alkali activated concretes includes the following parameters:

- pore solution (NaOH/KOH). Carbonation initially occurs in the pore solution of the concrete. Hence, NaOH/KOH as a dominant species in the pore solution plays a buffer role for the carbonation reactions;
- $\text{Ca(OH)}_2$  in the microstructure;
- Ca/Si in the microstructure.

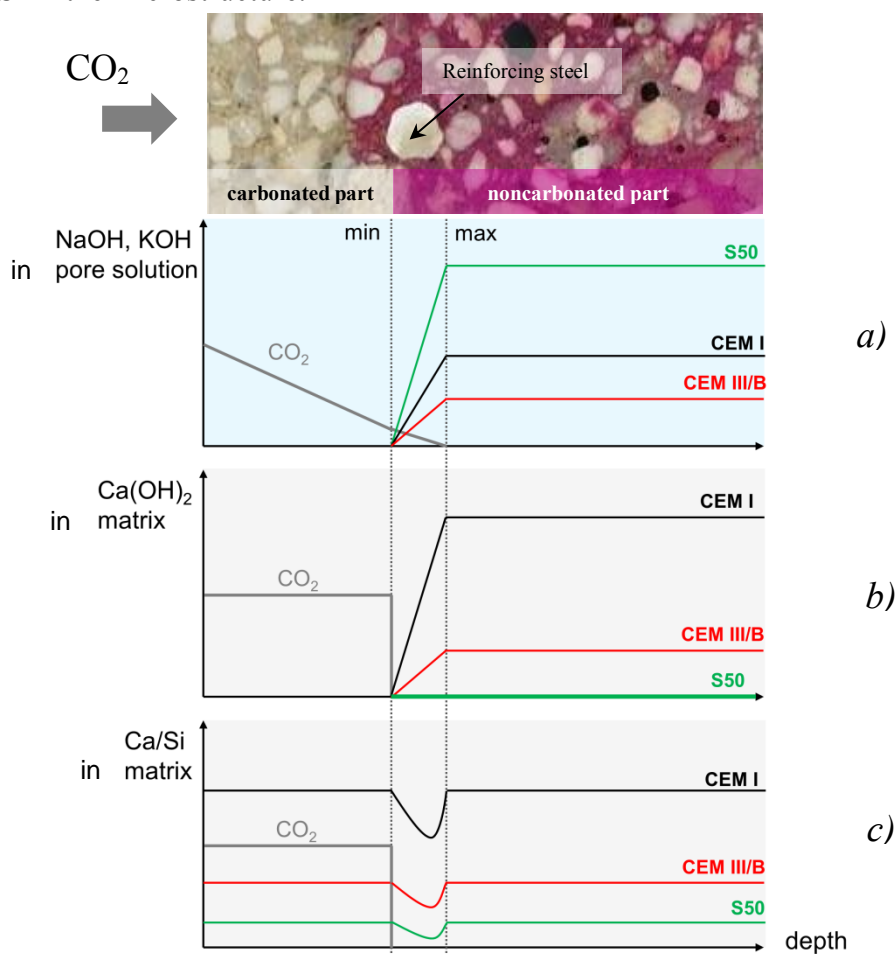


**Figure 1:** Domains (pore solution, microstructure) and parameters (NaOH/KOH,  $\text{Ca(OH)}_2$  content, Ca/Si ratio) for comparative study between CEM I and CEM III/B concretes and alkali activated concrete S50. The comparison includes the following:

- Pore solution (NaOH/KOH). Carbonation initially occurs in the pore solution of the concrete. Therefore, NaOH/KOH as a dominant species in the pore solution plays a buffer role for the carbonation reactions.
- $\text{Ca(OH)}_2$  in microstructure. Concrete CEM I has the highest content of  $\text{Ca(OH)}_2$ .
- Ca/Si in the microstructure. Concrete CEM I has the highest Ca/Si ratio.

A full understanding of the effects of these parameters on deterioration of concrete is a key step in modelling of the carbonation rate in alkali activated materials, as shown by Nedeljković [2]. According to Bernal et al. [3], the accelerated carbonation of the pore solution leads to significantly larger pH reduction (two pH log units lower) compared to natural carbonation. The pH in case of natural carbonation remains above 10. The reason why the pH is so high, is that the  $\text{Na}^+$  content remains constant regardless the partial pressure of  $\text{CO}_2$  [4]. The significant reduction of the pH in accelerated conditions is attributed to a higher fraction of bicarbonate ions ( $\text{HCO}_3^-$ ), which conditions are more acidic compared to carbonate ions ( $\text{CO}_3^{2-}$ ). This indicates that carbonation of the pore solution of alkali activated slag concrete would not be a problem in service conditions. However, there are no experimental measurements to validate numerical predictions. Furthermore, other mixtures than alkali activated slag concrete are not taken into account. To experimentally evaluate the effects of these parameters, in this paper the pH and carbonation depths are measured in alkali activated fly ash (FA) and ground granulated blast furnace slag (GGBFS) concrete and compared to cement-based concretes.

## 2. MATERIALS AND METHODS

### 2.1 Materials and sample preparation

Nedeljković et al. [5] shown that pastes with 100 wt.% GGBFS have a high resistance to carbonation due to their dense microstructures. It is of interest to study binders and concretes with lower slag content in the binder than 100 wt.%. For that purpose, the concretes with 50 wt.% GGBFS and 50 wt.% fly ash (FA) were cast (named S50 in the further text). Cement-based concretes were prepared with CEM I and CEM III/B. The details of mixtures proportions are listed in Table 1.

**Table 1:** Mixture designs for alkali activated concretes and cement-based concretes [ $\text{m}^3$ ].

	FA [kg]	GGBFS [kg]	CEM I [kg]	Aggregate [0-4 mm]	Aggregate [4-8 mm]	Aggregate [8-16 mm]	Activator [kg]	liquid/ binder
Density [ $\text{kg}/\text{m}^3$ ]	2440	2890	3000	2640	2650	2650	1250	[-]
Mix 1 S50	200	200	0	789.14	439.81	524.69	200	0.5
Mix 2 S50	130	130	0	789.14	439.81	524.69	156	0.6
Mix 3 CEM I	0	0	400	789.14	439.81	524.69	200 (water)	0.5
Mix 4 CEM III/B	0	280	120	789.14	439.81	524.69	200 (water)	0.5

In the absence of European standards for performance testing of alkali activated concrete, assessment for carbonation resistance are followed the EN 206-1 [6]. The assessment of carbonation resistance of alkali activated concrete with 260  $\text{kg}/\text{m}^3$  and 400  $\text{kg}/\text{m}^3$  of FA+GGBFS was performed to investigate conformity of an alkali activated concrete with minimum binder content for exposure class XC1 and XC3 [6], respectively.

The concrete samples were beams ( $1500 \times 100 \times 150 \text{ mm}^3$ ), which were cured in unsealed conditions (in curing room with 99% RH) for 28 days. After 28 days curing, the beams were sawn into 187.5-mm-wide samples (see Figure 2), sealed at the lateral sides and preconditioned for additional 28 days under laboratory conditions (55% RH, 20°C, 0.04% v/v  $\text{CO}_2$ ). After preconditioning, samples were exposed to different carbonation conditions (Table 2).

**Table 2:** Exposure conditions for carbonation of concretes.

	Natural laboratory	Natural outdoor	Accelerated carbonation
CO <sub>2</sub> concentration	0.04% v/v	0.04% v/v	1% v/v
Relative humidity	55%	80-98%	60%
Temperature	20°C	0-20°C	20°C

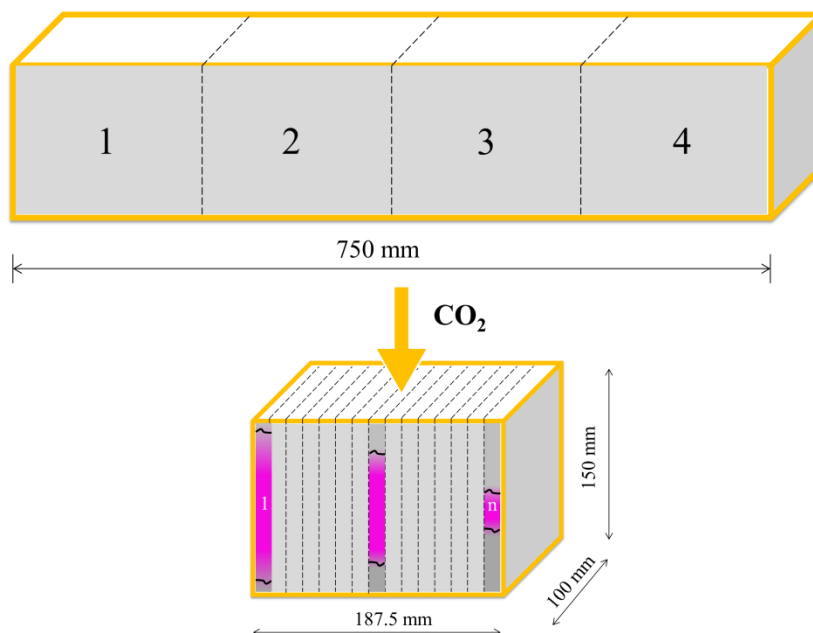


**Figure 2:** Geometry of the prepared concrete samples for each of the mixtures. After a certain period of exposure, a slice (width equal to 1 cm) of each of the prisms was cut (slices denoted as 1, ..., n). Subsequently, the slice surface was sprayed with phenolphthalein spray for measurement of the carbonation depth. The noncarbonated part is indicated by the pink colour.

## 2.2 Experimental methods

### 2.2.1 Compressive strength

Compressive strength was measured for each concrete mixture at 1 day, 7, 28, 56, 180, 365, 548 days according to the NEN 5988 on three cubes with dimension of 150×150×150 mm<sup>3</sup>. The mean values and standard deviations were calculated for each set of the data.

### 2.2.2 Carbonation depth

Carbonation depths were measured after 0, 14, 28, 42, 56, 114, 193, 236, 365, 548 days of exposure in accelerated conditions. In natural indoor and outdoor conditions, the carbonation depths were measured after 0, 28, 240, 365, 548. Slices with a thickness of 10-15 mm were cut from the concrete prisms by sawing (Figure 2). The fresh surface was sprayed with a 1 wt. % phenolphthalein aqueous solution. On average, 10 to 15 measurements were made per slice. Then the standard deviations were calculated for each set of the data.

### 2.2.3 pH of the pore solution

Direct extraction of the pore fluid from carbonated concrete samples was not possible due to the presence of aggregates and sample size that is needed for pore solution extraction. Therefore, pH measurements were carried out on simulated pore solutions, by equilibrating 1 g

of powdered sample with 10 ml of de-ionized water during 15 minutes at ambient temperature while stirring with a magnetic bar. Subsequently, the pH of the suspension was measured with a pH meter 827 Metrohm.

### 3. RESULTS AND DISCUSSION

#### 3.1 Compressive strength

The compressive strength results and standard deviations for alkali activated concretes S50 ( $l/b=0.5$ ), S50 ( $l/b=0.6$ ), cement-based concretes made of CEM I ( $w/c=0.5$ ) and CEM III/B ( $w/c=0.5$ ) are shown in Figure 3. The compressive strength of concretes was measured during curing, preconditioning and exposure. Afterwards, the concrete samples were placed in outdoor sheltered conditions, where development of the compressive strength was monitored from 56 days to 548 days.

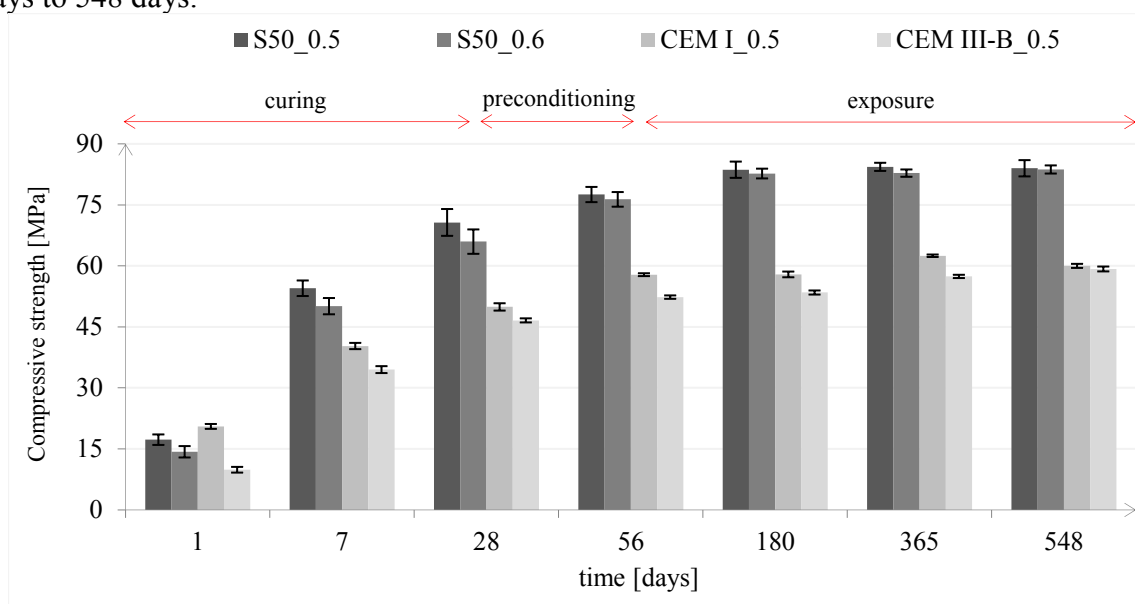


**Figure 3:** Compressive strength development in cement-based and alkali-activated concretes (samples  $(150 \times 150 \times 150 \text{ mm}^3)$  were cured in the curing room for 28 days, preconditioned for additional 28 days (28-56 days) at 55% RH and then exposed to natural outdoor sheltered conditions (56-548 days)).

Figure 3 shows that the strength of alkali-activated concrete samples is higher than that of cement-based concrete samples. Furthermore, when comparing compressive strength of S50 mixture with precursor content (GGBFS+FA) of  $400 \text{ kg/m}^3$  ( $l/b=0.5$ ) with S50 mixture with precursor content of  $260 \text{ kg/m}^3$  ( $l/b=0.6$ ), there is no significant difference, specifically at the later ages (180, 365, 548 days). This suggests that for reaching high strength in alkali-activated concrete, the binder content can be optimized, i.e. reduced. Exposure in natural outdoor conditions did not cause drop in compressive strength of the studied concretes.

#### 3.2 Carbonation depth

The propagation rate of the carbonation front was monitored for three exposure conditions: natural (outdoor (sheltered) and indoor) and accelerated carbonation conditions (Figure 4 (A), (B), (C)). Propagation of the carbonation front in concrete was monitored from the age of 56 days.

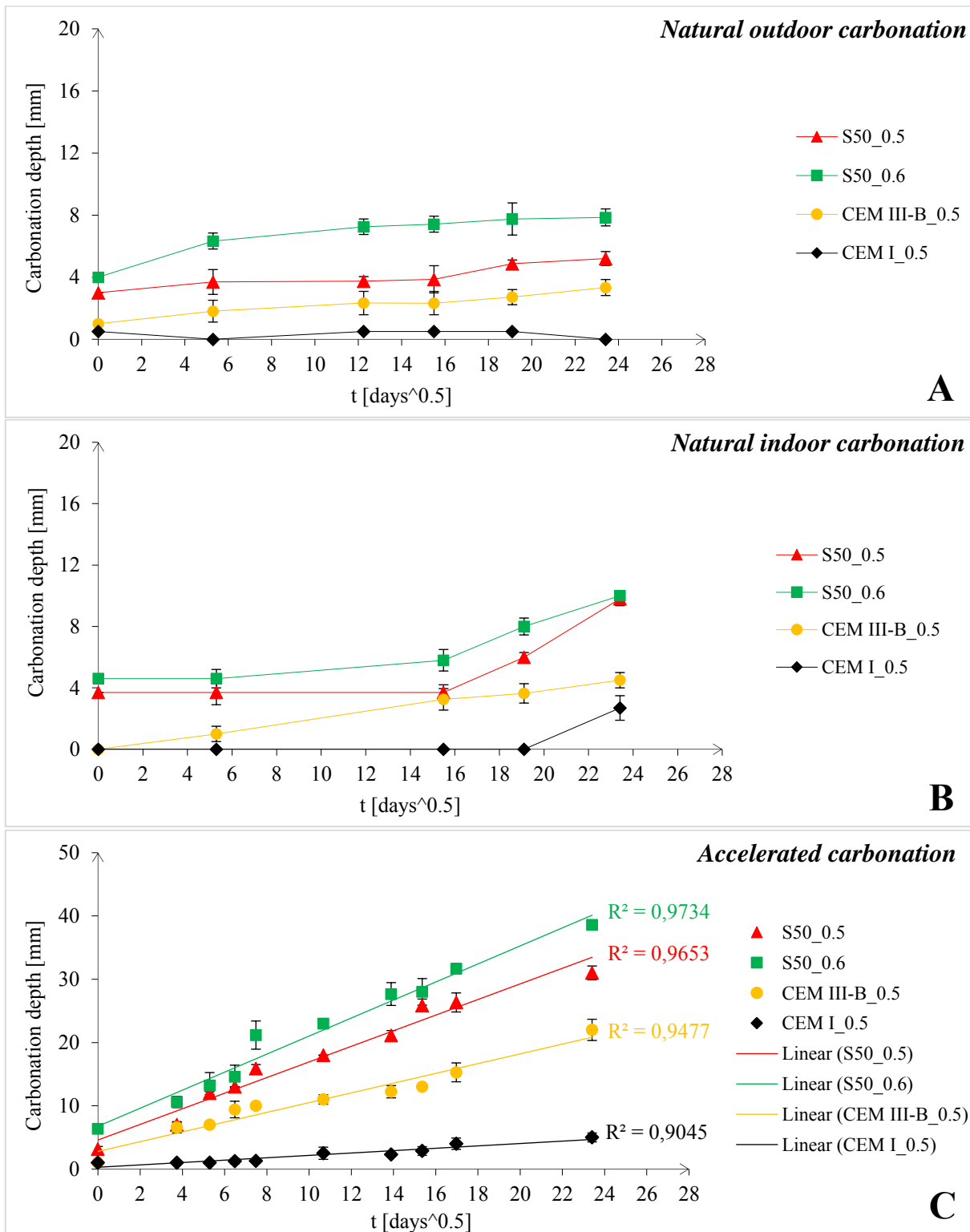


**Figure 4:** Carbonation depth versus time in natural outdoor (sheltered), indoor and accelerated carbonation conditions. At 56 days measurements of the carbonation depth in concretes started and, therefore 56<sup>th</sup> day is regarded as t=0. Since at 56 days carbonation depth was already measured, the fitted curves do not pass through the origin of the plots.

Figure 4 (A) demonstrates that carbonation did not proceed in the CEM I concrete in natural outdoor (sheltered) conditions. This is due to the large hydroxide alkalinity of the CEM I concrete. In contrast, the carbonation proceeds in CEM III/B and alkali activated concretes. For natural indoor conditions, sudden increase of carbonation depths can be seen after an age of 240 days (Figure 4(B)). The internal RH gradient over the cross section of the concrete sample at earlier stages can be an explanation for delayed carbonation of internal layers of the samples (4-12 mm).

Figure 4(C) indicates that in case of accelerated carbonation conditions, the propagation of the carbonation front is the fastest for the S50 ( $l/b=0.6$ ) mixture, followed by the S50 ( $l/b=0.5$ ), CEM III/B and CEM I. The carbonation is faster for S50 0.6 concrete, as  $l/b$  ratio is higher and the binder content is lower. CEM I 42.5 N concrete shows a high resistance to carbonation. Carbonation resistance decreases with decreasing clinker content, i.e. for CEM III/B 42.5 N concrete due to lower  $\text{Ca}(\text{OH})_2$  content, as shown by [7].

### 3.3 pH

The pH was also monitored for three different exposure conditions: natural (outdoor (sheltered) and indoor) and accelerated carbonation conditions (Figure 5 (A), (B), (C)). The pH of the pore solution in carbonated alkali-activated concrete is around 10, earlier than in cement-based concrete due to the absence of  $\text{Ca}(\text{OH})_2$ . However, the phenolphthalein indicator shows that a gradual color change of phenolphthalein from fuchsia to colorless upon pH changes from 10 to 8.2. Therefore, it cannot be stated that the pore solution of alkali-activated concrete is neutralized to 8.2, since it can also be reduced to maximum pH 10 and again it appears as colourless. The pH of the carbonated alkali-activated concrete in accelerated test is found to be higher than 9. Due to the absence of  $\text{Ca}(\text{OH})_2$  in alkali-activated concretes, the  $\text{CO}_2$  diffusion and  $\text{CO}_2$  binding capacity of the mixture S50, are the subsequent mechanisms for faster propagation of the carbonation front compared to the cement-based concretes. In the case of natural carbonation (indoor and outdoor), the pH values are very close for all concretes (see Figure 5 (A), (B)).

According to the pH values, after 548 days of exposure, three stages can be distinguished for alkali activated concretes in case of accelerated carbonation (see Figure 5 (C)):

(1) from 0 mm to 15 mm, the pH of concrete surface decreases to 9.2, where the alkalis are fully depleted. This zone is fully carbonated;

(2) from 30 mm to 15 mm, the pH of concrete decreases from 10.20 to 9.6. This suggests that the alkalis are partially depleted. This zone is partially carbonated;

(3) from 30 mm to 40 mm, the pH of concrete is above 10. This zone is noncarbonated.

In case of natural carbonation, only stages (1) and (3) are observed. This indicates slow progress of the carbonation process in natural conditions. Nevertheless, the pH in stage (1) in natural conditions is similar to stage (1) for accelerated carbonation. The pH in stage (1) and (2) of carbonated alkali activated concrete corresponds well with the pH of alkali activated pastes after 500 days of accelerated carbonation, as shown by Nedeljković et al. [8].

The pH of the CEM I concrete is maintained around 10.5. This value, however, is not a true pH especially not for the carbonated cement-based concrete (Figure 5 (C)). Some  $\text{Ca}(\text{OH})_2$  remains after carbonation and it dissolves when the suspension is made. Therefore, the pH evaluation using suspension method is not appropriate for CEM I concrete.

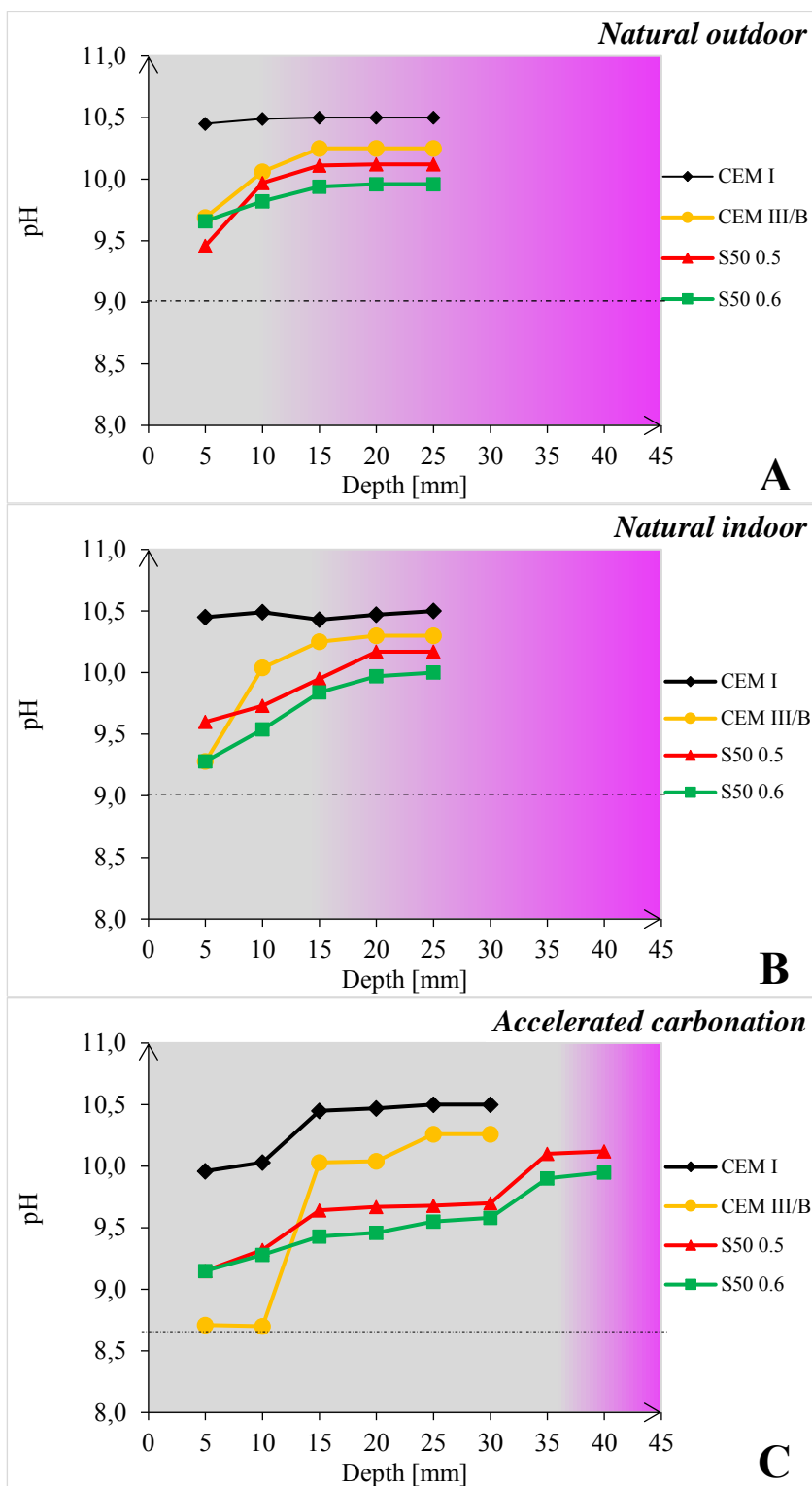


**Figure 5:** pH along carbonation path measured after 548 days of exposure in natural (indoor and outdoor (sheltered)) and accelerated carbonation conditions. (In the graphs, pink colour indicates noncarbonated zone and grey colour indicates the carbonated zone.)



For CEM III/B concrete, the results reflect the real reduction of the pH under carbonation.  $\text{Ca}(\text{OH})_2$  in CEM III/B concrete is mainly consumed by the pozzolanic reaction of GBFS. Therefore, the only source of alkalis after carbonation of this type of concrete are  $\text{Na}^+$  and  $\text{K}^+$ . Under accelerated carbonation conditions, the carbonated CEM III/B concrete has a pH below 9, while in the noncarbonated part a pH  $>10$  is measured. In natural indoor and outdoor conditions of exposure, the pH of carbonated CEM III/B concrete is above 9.

The pH of all carbonated alkali-activated S50 concretes was above the pH 9, which is reported as a threshold value for an initiation of the carbonation induced reinforcement corrosion in the OPC-based binders [9]. The pH of the noncarbonated alkali-activated concretes S50 was above 10.

#### 4. CONCLUSIONS

- The higher propagation rate of the carbonation front in the alkali-activated GGBFS+FA concrete, despite its higher compressive strength and finer pore structure compared to cement-based concrete, is due to absence of  $\text{Ca}(\text{OH})_2$ , different pore solution chemistry (alkalinity buffer), lower calcium content in the gel phases, hence lower content of the carbonatable phases.
- From all above factors, the carbonation rate is the most influenced by the alkalinity of the alkali activated concretes. This implies that the total alkalinity of the material might be used in future to predict the carbonation depths. It should be noted that the carbonation depth for alkali activated concrete is the domain where alkalinity is reduced and microstructure is deteriorated.
- Improved carbonation resistance of the alkali-activated concrete S50 can be achieved by higher GGBFS content (70, 100 wt.%) and by applying the sealed curing.
- Future modeling studies are needed to consider the synergy between reduced alkalinity and deterioration of concrete microstructure under different exposure conditions.

#### REFERENCES

- [1] Arbi, K., Nedeljković, M., Zuo, Y. and Ye, G. ‘A review on the durability of alkali-activated fly ash/slag systems: advances, issues, and perspectives’ *Ind. Eng. Chem. Res.*, **55**(19)(2016) 5439-5453.
- [2] Nedeljković, M. *Carbonation mechanism of alkali-activated fly ash and slag materials: In view of long-term performance predictions*. Ph.D. Thesis, Delft: Delft University Press, 2019.
- [3] Bernal, S. A., Provis, J. L., Brice, D. G., Kilcullen, A., Duxson, P. and van Deventer, J. S. ‘Accelerated carbonation testing of alkali-activated binders significantly underestimates service life: The role of pore solution chemistry.’ *Cem. Concr. Res.* **42**(10)(2012) 1317-1326.
- [4] Bernal, S. A., de Gutierrez, R. M., Provis, J. L. and Rose, V. ‘Effect of silicate modulus and metakaolin incorporation on the carbonation of alkali silicate-activated slags.’ *Cem. Concr. Res.* **40**(6)(2010) 898-907.
- [5] Nedeljković, M., Zuo, Y., Arbi, K. and Ye, G. ‘Carbonation resistance of alkali-activated slag under natural and accelerated conditions.’ *Journal of Sustainable Metallurgy* **4**(1)(2018), 33-49.
- [6] EN 206-1 Concrete - Part 1: Specification, performance, production and conformity (CEN, 2013).
- [7] Nedeljković, M., Ghiassi, B., Melzer, S., Kooij, C., van der Laan, S. and Ye, G. ‘CO<sub>2</sub> binding capacity of alkali-activated fly ash and slag pastes.’ *Ceram. Int.* **44**(16)(2018), 19646-19660.
- [8] Nedeljković, M., Ghiassi, B., van der Laan, S., Li, Z. and Ye, G. ‘Effect of curing conditions on the pore solution and carbonation resistance of alkali-activated fly ash and slag pastes’ *Cem. Concr. Res.* **116**(2019) 146-158.
- [9] Bertolini, L., Elsener, B., Pedferri, P., Redaelli, E. and Polder, R. ‘Carbonation-Induced Corrosion’ in *Corrosion of Steel in Concrete*, Wiley-VCH Verlag GmbH & Co. KGaA, 2013, 79-92.